

AN ASSEMBLAGE OF BISMUTH-RICH, TELLURIUM-BEARING MINERALS IN THE EL QUEMADO GRANITIC PEGMATITE, NEVADOS DE PALERMO, SALTA, ARGENTINA

MARÍA FLORENCIA MÁRQUEZ-ZAVALÍA[§] AND MIGUEL Á. GALLISKI

IANIGLA, CCT-MENDOZA CONICET, Avda. Ruiz Leal s/n, Parque Gral. San Martín, C.C.330 (5.500) Mendoza, Argentina

PETR ČERNÝ AND RON CHAPMAN

Department of Geological Sciences, University of Manitoba, Winnipeg, Manitoba R3T 2N2, Canada

ABSTRACT

An assemblage of bismuth-rich, tellurium-bearing minerals in the El Quemado pegmatite, Salta, Argentina, represents late-stage mineralization in a spodumene-subtype, rare-element class granitic pegmatite. The minerals occur in an irregular, volumetrically minor core-margin association, dominated by fine-grained muscovite and quartz, with accessory U-rich fluorinatromicrolite, zircon, bismuth, bismuthinite, emplectite, hodrušite, and the sulfotellurides joséite-A, joséite-B, tetradymite and ingodite. Early bismuth is replaced by abundant bismuthinite, which also locally contains symplectitic intergrowths of emplectite ($\text{Cu}_{1.02}\text{Bi}_{0.98}\text{S}_{2.00}$). A single euhedral crystal of hodrušite [$(\text{Cu}_{4.04}\text{Fe}_{0.12}\text{Ag}_{0.03})_{\Sigma 4.19}(\text{Bi}_{15.87}\text{Pb}_{0.02})_{\Sigma 5.89}\text{S}_{10.92}$] has Pb-bearing tips that contain 3.62 to 4.39 wt.% Pb (0.33 to 0.40 *apfu* respectively). Joséite-A ($\text{Bi}_{4.04}\text{Te}_{0.95}\text{S}_{2.01}$) forms an intergrowth with ingodite, enclosed in emplectite. Joséite-B ($\text{Cu}_{0.02}\text{Bi}_{4.01}\text{Te}_{1.93}\text{S}_{1.04}$) is intergrown with joséite-A and with bismuthinite in emplectite. Tetradymite [$(\text{Bi}_{2.00}\text{Cu}_{0.02})_{\Sigma 2.02}\text{Te}_{1.95}\text{S}_{1.03}$] is included in emplectite and bismuthinite. Ingodite is usually enclosed in bismuthinite as very small grains with a composition $\text{Bi}_{1.98}\text{Te}_{1.00}\text{S}_{1.02}$. Late-stage or supergene alteration of this association generated fairly abundant bismutite and rare bismite. On the basis of experimental data, the equilibrium association of bismuth, bismuthinite, emplectite and hodrušite, typical of hydrothermal ore deposits but uncommon in granitic pegmatites, is restricted to relatively low temperatures and a pressure in the range 2–3 kbar.

Keywords: granitic pegmatite, bismuth, bismuthinite, emplectite, hodrušite, joséite-A, joséite-B, tetradymite, ingodite, El Quemado, Salta, Argentina.

INTRODUCTION

The sulfide minerals of Bi are relatively common as minor phases in granitic pegmatites, particularly in the most diversified rare-element pegmatites of the more common petrogenetic families, LCT (Li–Cs–Ta) and NYF (Nb–Y–F). Among the LCT pegmatites, Tanco, Canada has a vast array of native elements, alloys, sulfides and sulfosalts (Černý & Harris 1978). In the same petrogenetic family, the Rubikon and especially the Swartberg pegmatites of southern Africa (Ciobanu & Cook 2002) contain aikinite, bismuthinite, wittichenite, emplectite, berryite and hodrušite, and padérite, gladite, bismuthinite, emplectite and joséite-A, respectively. Among pegmatites of the NYF petrogenetic family, a complex association of Bi minerals

forms cuprobismutite homologues in pegmatites at Szklarska Poręba, Poland (Pieczka & Gołębioska 2012). In the granitic pegmatites of Argentina, the most common primary phases distributed in pegmatites of beryl–columbite–phosphate type or spodumene subtype are bismuth and bismuthinite. Also, isolated grains of tetradymite were described in a pegmatite of probable NYF affiliation at Cerro Blanco, Córdoba (Ahlfeld & Olsacher 1944, Rivas 1969). More recently, Galliski (1983b) briefly described an assemblage of bismuth minerals from the El Quemado spodumene-subtype granitic pegmatite, consisting of bismuth, bismuthinite, emplectite, wittichenite, Bi-rich tennantite, and bismutite. His mineral identification was mainly based on the X-ray powder-diffraction patterns and optical properties of these minerals. In this contribution, we

[§] E-mail address: mzavalia@mendoza-conicet.gov.ar

re-examine this paragenesis and document the chemical compositions of the minerals by electron-microprobe analysis.

OCCURRENCE

The El Quemado pegmatite is located at $\sim 66^{\circ}21' 14''$ S and $24^{\circ}51' 2''$ W, at $\sim 4,685$ m above sea level, in the Nevados de Palermo mountain range, Salta Province, Argentina (Fig. 1). The best access to the pegmatite is from Palermo Viejo, a two-day trek on horseback. El Quemado is a complex rare-element pegmatite of the spodumene subtype, according to the classification of Černý & Ercit (2005). The pegmatite is part of the El Quemado pegmatite field, the northernmost in the Pampean pegmatite province (Galliski 1994). The bodies of pegmatite were emplaced into a monotonous Upper Precambrian to Lower Paleozoic metapelite–metagreywacke sequence that had undergone low- to medium-grade metamorphism (Galliski 1983a). This sequence was intruded during the Ordovician by a suite of I-type trondhjemites (Galliski & Miller 1989, Galliski *et al.* 1990) and a few small cupolas of S-type peraluminous granites and pegmatites (Galliski 2007). The El Quemado pegmatite, together with the other major pegmatites of this field (Santa Elena, Tres Tetos and Anzotana) yielded more than 10 t of tantalum ore and 5 t of bismuth ore concentrates in the 1940s (Galliski 1983b).

The geology of El Quemado pegmatite field was described by Galliski (1983b); we summarize here the major characteristics of the El Quemado pegmatite. Outcrops of this pegmatite are very scarce, exposed on a steep slope near the top of a drainage divide. At the time of sampling, only three small outcrops of the pegmatite were not covered by detritus. The El Quemado pegmatite is ~ 40 m long in outcrop and it is at least 6 m thick; it strikes $N40^{\circ}W$ and steeply dips to the

southwest. The host rock is a cordierite-bearing mica-schist that strikes $N50^{\circ}E$ and dips $60^{\circ}NW$. Five zones (Fig. 2) are well defined [following the terminology and criteria of Cameron *et al.* (1949)]. The border zone (a) is 5 cm thick, fine-grained and composed of albite and quartz, with accessory muscovite, fluorapatite, montebrasite, epidote, tantalite-(Mn) and altered triphylite. The medium-grained wall zone (b) consists of quartz, albite and muscovite, with accessory tantalite-(Mn), fluorapatite and eosphorite. The coarse-grained outer intermediate zone (c) is composed of K-feldspar, albite, quartz and muscovite, with accessory tantalite-(Mn); along one side of the pegmatite, this zone becomes almost monomineralic, with coarse-grained quartz resembling an asymmetrically positioned quartz core. The inner intermediate zone (d) consists of spodumene and quartz, with minor montebrasite and pink muscovite. The assemblage interpreted as forming along the core margin (e) is composed of fine-grained muscovite and quartz, with U-rich fluornatromicrolite, zircon and minerals of Bi and Te.

The Bi and Te minerals examined here constitute irregular aggregates, up to 2 cm long, with predominant native bismuth and bismuthinite. They are usually enclosed in quartz or quartz and muscovite. In the past, pods of bismuth minerals weighing up to 20 kg were reported from the El Quemado district (Ahlfeld & Angelelli 1948).

ANALYTICAL METHODS

The specimens were prepared as conventional polished sections, and studied under a polarizing reflected-light microscope. Chemical analyses of the minerals were performed with a CAMECA SX-50 electron microprobe, using an accelerating voltage of 15 kV, a beam current of 20 nA measured on a Faraday cup, a counting time 20 s for each element and 10 s for

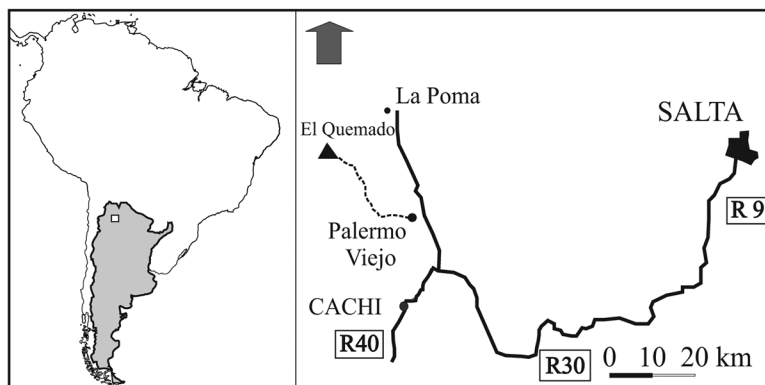


FIG. 1. Location of El Quemado pegmatite in northern Argentina.

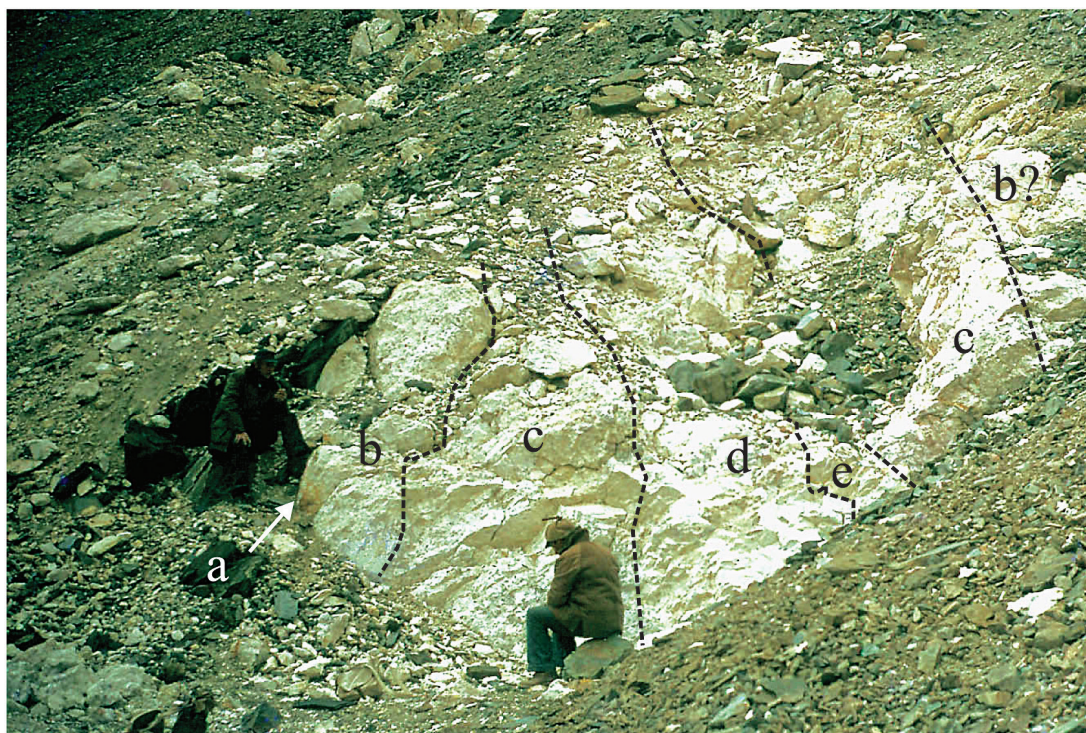


FIG. 2. The main quarry of the El Quemado pegmatite viewed from the southeast: (a) border zone, (b) wall zone, (c) outer intermediate zone, (d) inner intermediate zone, (e) core-margin zone.

the background, with a beam diameter of 2 μm . The standards and analytical lines selected were as follows: S (CuFeS₂, K α), Cu (CuFeS₂, K α), Fe (CuFeS₂, K α), Mn²⁺ [Mn₃Al₂(SiO₄)₃, K α], Ni (Ni₉S₈, K α), Zn (ZnS, K α), Au (Au₁₀₀, M α), Ag (Au₆₀Ag₄₀, L α), In and As (InAs, L α), Sn (SnO₂, L α), Sb (Sb₂Te₃, L α), Te (Sb₂Te₃, L α), Pb (PbS, M α), Bi (Bi₂Se₃, M β) and Se (Bi₂Se₃, L α). Two of the three original polished sections used to perform these analyses (#1383 and 1384) were lost at the University of Manitoba, which precluded any additional analyses. New polished sections prepared with remnant samples of lower quality were used for new analytical work. The additional chemical analyses of some sulfide and sulfosalts minerals were performed at the Universidad Nacional de Córdoba, Argentina, with a JEOL JXA-8200 Superprobe electron microprobe, with a beam diameter of 2 μm and an acceleration potential of 15 kV. We used a sample current of 20 nA measured on a Faraday cup and counting times of 20 s for the element and 10 s for the background. The standards and analytical lines selected were as follows: Ag (silver, L α), Pb (galena, M α), S (chalcopyrite, K α), Cu (chalcopyrite, K α), Te (coloradoite, L α), Bi (bismuthinite, M β). The data were reduced using the PAP routine of Pouchou & Pichoir (1985). The chemical

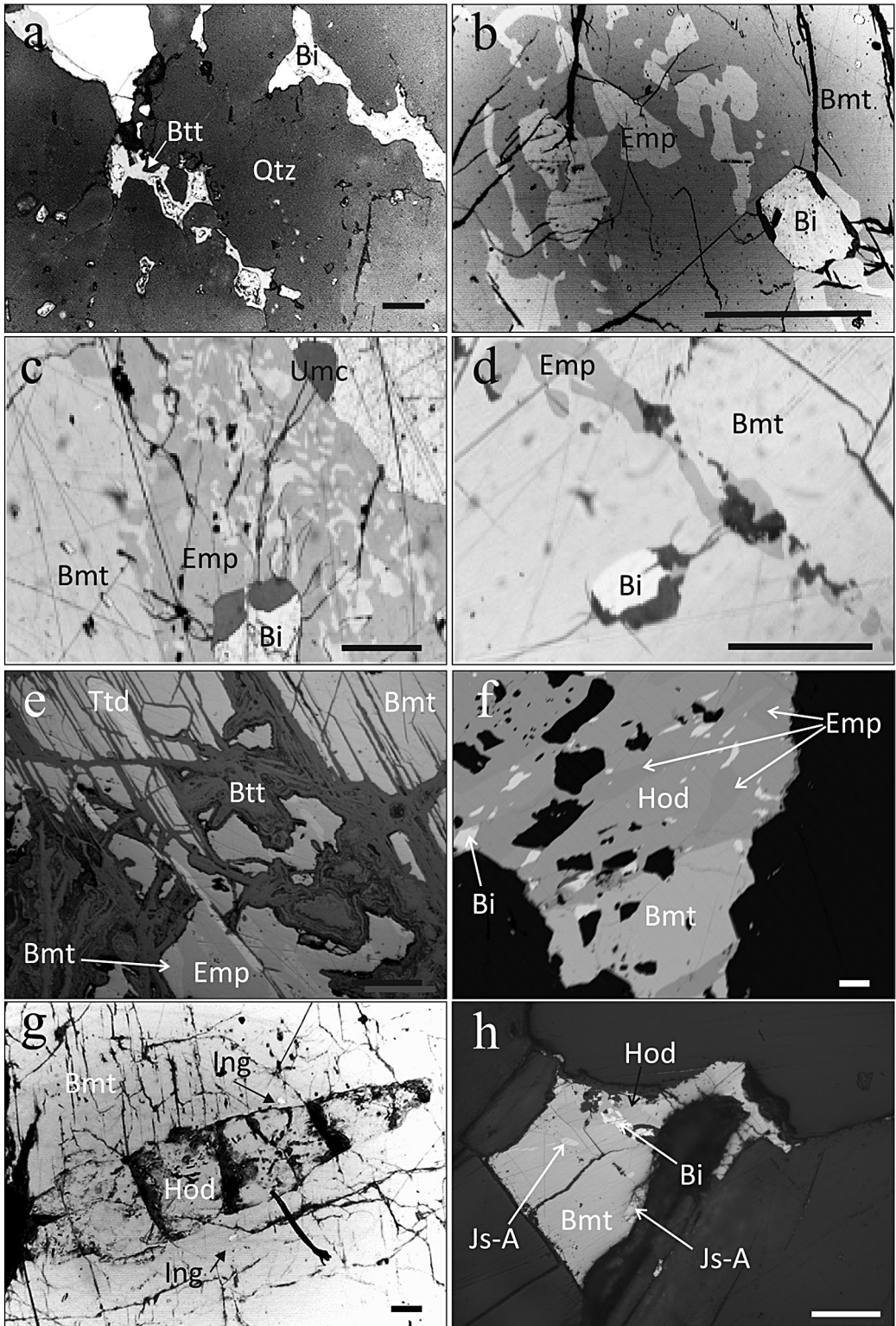
compositions and formulae of the analyzed minerals are shown in Table 1.

THE BISMUTH- AND TELLURIUM-BEARING MINERALS

The diverse assemblages of Bi- and Te-bearing minerals in El Quemado pegmatite include native bismuth, bismuthinite, emplectite, hodrušite (including hodrušite unusually rich in Pb), joséite-A, joséite-B, tetradymite, ingodite, and products of their alteration, bismutite and bismite.

Bismuth occurs as widespread irregular grains enclosed in quartz (Fig. 3a) or fine-grained muscovite, from 1 μm to 5 mm in size. Bismuth was also found as irregular grains ($\leq 20 \mu\text{m}$) in bismuthinite (Fig. 3b), intergrown with emplectite; late peripheral replacement of bismuth by bismuthinite also is common. Bismuth is also replaced by a late generation of a U-rich member of the microlite group, which upon metamictization generated fractures that crisscross the adjacent minerals (Fig. 3c). Electron-microprobe analyses gave 99.57 to 100.17 wt.% Bi, and only traces of Cu, Pb, Sb and S.

Bismuthinite is more abundant than bismuth and occurs as irregular aggregates in quartz. Symplectically intergrown with emplectite, it hosts U-rich



fluornatromicrolite and relics of bismuth (Figs. 3b, c), and is associated with the other Bi-rich minerals of the assemblage. The average composition ($n = 15$) shown in Table 1 leads to the structural formula $\text{Bi}_{1.99}\text{Cu}_{0.03}\text{S}_{2.98}$. Some of the grains show compositions with small quantities of other elements such as Cu, Ag and Pb, but in all cases their concentrations are <0.5 wt.%.

Small single grains (≤ 4 mm) of *empletite* are enclosed in quartz or associated with bismuthinite. *Empletite* hosts inclusions of metamict U-rich fluornatromicrolite and a few relics of bismuth (Fig. 3c), develops intergrowths with bismuthinite (Fig. 3d) in places, and contains exsolution-induced domains of tetradymite (Fig. 3e). The average of 12 analyses (Table 1) gave the empirical formula $\text{Cu}_{1.02}\text{Bi}_{0.98}\text{S}_{2.00}$.

Hodrušite is intergrown with *empletite* (Fig. 3f). It is also associated with bismuthinite (Figs. 3g, h). Figure 3g shows a single pale brownish grey, arrowhead-shaped crystal 900 μm long and up to 200 μm wide, enclosed in bismuthinite. This crystal shows parting perpendicular to its length, and possibly a cleavage in one direction parallel to the elongation, as suggested by uniformly aligned strings of secondary bismuthite grains (up to 20 by 2 μm). *Hodrušite* is softer than bismuthinite, has distinctive pleochroism and birefractance, and a strong anisotropy in violet-grey and creamy pinkish pale grey; no internal reflections are visible.

The chemical composition of the central part of the crystal plots in the (Cu + Fe) – (Bi + Ag) – (Pb + Cd) space, close to *hodrušite* (Fig. 4a), whereas both extremities are significantly enriched in Pb but far from the compositional field of *padérite* (Fig. 4b); the structural formula, calculated from the average of 10 analyses shown in Table 1, is $(\text{Cu}_{4.04}\text{Fe}_{0.12}\text{Ag}_{0.03})_{\Sigma 4.19}(\text{Bi}_{5.87}\text{Pb}_{0.02})_{\Sigma 5.89}\text{S}_{10.92}$. The areas enriched in Pb, with up to 4.39 wt.% Pb (0.40 *apfu*), give the following empirical formula, calculated from the average result

of four analyses: $(\text{Cu}_{3.74}\text{Fe}_{0.02})_{\Sigma 3.76}(\text{Bi}_{5.71}\text{Pb}_{0.37})_{\Sigma 6.08}(\text{S}_{11.15}\text{Sb}_{0.01})_{\Sigma 11.16}$.

Joséite-A forms scarce blade-shaped grains up to 30 μm in size hosted by *empletite*, and rounded to irregular inclusions in bismuthinite (Fig. 3h). The structural formula calculated from the average of the representative compositions shown in Table 1 and based on 7 *apfu* is $\text{Bi}_{4.04}\text{Te}_{0.95}\text{S}_{2.01}$.

Joséite-B forms small anhedral grains, up to 25 μm across. Its color is white with a weak creamy hue; birefractance is very weak, in some cases indiscernible. Reflectivity is high, slightly higher than for *joséite-A*. *Joséite-B* is softer than its host, *empletite*, and lacks evidence of cleavage. Anisotropy is distinct, with bluish grey to brownish colors. *Joséite-B* is found enclosed in *empletite*, intergrown with *joséite-A*, and with small inclusions of bismuthinite; some grains of *joséite-B* are replaced along their borders by bismuthite. The empirical formula, calculated from the average result of six analyses (Table 1) is $\text{Cu}_{0.02}\text{Bi}_{4.01}\text{Te}_{1.93}\text{S}_{1.04}$.

Tetradymite is scarce, associated with *empletite* and bismuthinite in elongate inclusions. It shows optical properties that are typical of the species. Its structural formula, calculated from the average of five chemical analyses (Table 1) and based on five atoms per formula unit (*apfu*) is $(\text{Bi}_{2.00}\text{Cu}_{0.02})_{\Sigma 2.02}\text{Te}_{1.95}\text{S}_{1.03}$.

Ingodite is the scarcest of the minerals in this association. It forms small anhedral grains up to 25 μm across in bismuthinite (Fig. 3g). Its color is pure white, with high reflectivity and weak to moderate birefractance. *Ingodite* is softer than its host bismuthinite and lacks cleavage. Anisotropy is strong, from bluish grey to bright creamy white, and no internal reflections are observed. This mineral is slightly nonstoichiometric, with $[\text{Bi}/(\text{S} + \text{Te})] = 0.98$ and a Te:S ratio in the range 0.495–0.505, well in accordance with the range reported by Cook *et al.* (2007). The structural formula, calculated from the composition shown in Table 1, is $\text{Bi}_{1.98}\text{Te}_{1.00}\text{S}_{1.02}$.

Bismuthite commonly replaces bismuth and bismuthinite along their borders or along cleavage or parting planes (Fig. 3e). A banded texture is locally developed. *Bismuthite* also occurs as patches and thin veinlets in bismuthinite. The analysis gave 82.26 wt.% Bi, equivalent to 91.71 wt.% Bi_2O_3 ; the stoichiometric proportion of CO_2 fitting the formula $\text{Bi}_2(\text{CO}_3)_2\text{O}_2$ would be 8.66 wt.%, giving a total of 100.37 wt.%.

Bismite is very scarce and was found only as an alteration product after bismuth.

DISCUSSION

In the El Quemado pegmatite, the late-stage system that generated the assemblage examined was dominated by Bi, Cu and S, with traces of Pb, Fe and Te. Textural relationships indicate that the paragenetic sequence of the primary phases is native bismuth, bismuthinite, *empletite*, *hodrušite*, *joséite-A*, *joséite-B*, tetradymite

FIG. 3. Back-scattered electron images (a, b, f, g) and photomicrographs (c, d, e, h) of (a) bismuth in interstices of quartz, in part replaced by bismuthite, (b) symplectitic intergrowths of bismuthinite and *empletite*, (c) bismuth partially replaced by U-rich fluornatromicrolite and enclosed in bismuthinite intergrown with *empletite*, (d) a crystal of bismuth enclosed in bismuthinite intergrown with *empletite*, (e) bismuthinite partially altered to bismuthite and intergrown with *empletite* with exsolution-induced domains of tetradymite, (f) bismuthinite associated with *hodrušite*-bearing *empletite* exsolution-induced domains and bismuth, (g) an arrowhead-shaped crystal of *hodrušite* and two small inclusions of *ingodite* enclosed in bismuthinite, (h) exsolution-induced domains of *joséite A* in bismuthinite associated with *hodrušite*. The scale bar is 50 μm in all images. Bi: bismuth, Bmt: bismuthinite, Btt: bismuthite, Emp: *empletite*, Hod: *hodrušite*, Ing: *ingodite*, Js-A: *joséite-A*, Qtz: quartz, Ttd: tetradymite, Umc: U-rich fluornatromicrolite.

TABLE 1. CHEMICAL COMPOSITIONS OF THE BISMUTH MINERALS AT EL QUEMADO

	Cu	Fe	Pb	Ag	Bi	Sb	Te	S	Total	Calculated formula
Bismuth										
Mean $n = 4$	0.01	0.00	0.01	n.a.	99.98	0.03	0.00	0.08	100.32	$\text{Bi}_{0.99}\text{S}_{0.01}$
σ		0.00	0.00	0.00	---	0.18	0.00	0.00	0.07	
Bismuthinite										
Mean $n = 15$	0.36	0.02	0.35	0.01	81.25	0.00	0.01	18.66	100.04	$\text{Bi}_{1.99}\text{Cu}_{0.03}\text{S}_{2.98}$
σ		0.38	0.00	1.13	0.01	1.13	0.00	0.01	1.69	
Emplectite										
1384-14	18.86	0.04	0.00	n.a.	61.37	0.30	0.00	19.31	99.98	$\text{Cu}_{0.99}\text{Bi}_{0.98}(\text{S}_{2.01}\text{Sb}_{0.01})\Sigma 2.02$
Q5-022	19.08	n.a.	0.00	0.00	62.11	n.a.	0.00	19.04	100.23	$\text{Cu}_{1.01}\text{Bi}_{1.00}\text{S}_{1.99}$
Q5-023	19.28	n.a.	0.00	0.02	62.45	n.a.	0.00	19.10	100.85	$\text{Cu}_{1.01}\text{Bi}_{1.00}\text{S}_{1.99}$
Q5-024	19.08	n.a.	0.00	0.05	61.55	n.a.	0.00	19.30	99.98	$\text{Cu}_{0.99}\text{Bi}_{0.99}\text{S}_{2.01}$
Q5-026	18.77	n.a.	0.03	0.05	62.44	n.a.	0.00	19.11	100.40	$\text{Cu}_{1.00}\text{Bi}_{2.00}\text{S}_{2.00}$
Q7-059	19.71	n.a.	0.00	0.00	61.08	n.a.	0.00	19.36	100.15	$\text{Cu}_{1.03}\text{Bi}_{0.97}\text{S}_{2.00}$
Q8-061	19.69	n.a.	0.00	0.00	61.71	n.a.	0.00	19.61	101.00	$\text{Cu}_{1.02}\text{Bi}_{0.97}\text{S}_{2.01}$
Q8-062	19.63	n.a.	0.07	0.07	61.26	n.a.	0.00	19.22	100.24	$\text{Cu}_{1.03}\text{Bi}_{0.98}\text{S}_{1.99}$
Q8-063	19.50	n.a.	0.00	0.18	62.05	n.a.	0.00	19.41	101.14	$\text{Cu}_{1.02}\text{Bi}_{0.98}\text{S}_{2.00}$
Q8-064	19.77	n.a.	0.00	0.14	61.88	n.a.	0.00	19.37	101.16	$\text{Cu}_{1.03}\text{Bi}_{0.98}\text{S}_{1.99}$
Q8-065	19.38	n.a.	0.00	0.08	62.62	n.a.	0.00	19.41	101.50	$\text{Cu}_{1.01}\text{Bi}_{0.99}\text{S}_{2.00}$
Q8-076	19.84	n.a.	0.05	0.01	61.76	n.a.	0.00	19.20	100.86	$\text{Cu}_{1.03}\text{Bi}_{0.98}\text{S}_{1.99}$
Mean $n = 12$	19.49	0.00	0.01	0.05	61.86	0.00	0.00	19.33	100.26	$\text{Cu}_{1.02}\text{Bi}_{0.98}\text{S}_{2.00}$
σ		2.32	0.00	0.01	0.04	2.70	0.00	0.00	0.59	
Hodrušite										
1384-15	13.79	0.38	0.00	n.a.	66.92	0.07	0.00	19.52	100.79	$(\text{Cu}_{3.98}\text{Fe}_{0.13}\text{Zn}_{0.03})\Sigma 4.14\text{Bi}_{5.66}(\text{S}_{11.16}\text{Sb}_{0.01})\Sigma 11.17$
1384-21	14.08	0.25	0.00	n.a.	66.92	0.00	0.00	18.96	100.21	$(\text{Cu}_{4.14}\text{Fe}_{0.08})\Sigma 4.22\text{Bi}_{5.73}\text{S}_{11.05}$
1384-23	14.17	0.35	0.00	n.a.	66.66	0.00	0.00	19.09	100.27	$(\text{Cu}_{4.14}\text{Fe}_{0.12})\Sigma 4.26\text{Bi}_{5.67}\text{S}_{11.07}$
1384-28	13.82	0.40	0.00	n.a.	66.36	0.00	0.00	19.19	99.77	$(\text{Cu}_{4.05}\text{Fe}_{0.13}\Sigma 4.18\text{Bi}_{5.66}\text{S}_{11.16}$
1384-30	13.28	0.51	0.00	n.a.	66.80	0.00	0.00	19.15	99.74	$(\text{Cu}_{3.92}\text{Fe}_{0.17})\Sigma 4.09\text{Bi}_{5.72}\text{S}_{11.19}$
Q5-016	13.34	n.a.	0.42	0.15	67.45	n.a.	0.00	18.95	100.30	$(\text{Cu}_{3.91}\text{Ag}_{0.03})\Sigma 3.94(\text{Bi}_{6.01}\text{Pb}_{0.04})\Sigma 6.05\text{S}_{11.01}$
Q6-035	14.26	n.a.	0.43	0.31	66.44	n.a.	0.00	18.95	100.39	$(\text{Cu}_{4.14}\text{Ag}_{0.03})\Sigma 4.19(\text{Bi}_{5.66}\text{Pb}_{0.04})\Sigma 5.90\text{S}_{10.91}$
Q6-036	13.94	n.a.	0.41	0.31	66.91	n.a.	0.00	19.09	100.66	$(\text{Cu}_{4.04}\text{Ag}_{0.05})\Sigma 4.09(\text{Bi}_{5.90}\text{Pb}_{0.04})\Sigma 5.94\text{S}_{10.97}$
Q6-037	13.99	n.a.	0.36	0.38	65.99	n.a.	0.00	18.95	99.66	$(\text{Cu}_{4.08}\text{Ag}_{0.07})\Sigma 4.15(\text{Bi}_{5.86}\text{Pb}_{0.03})\Sigma 5.89\text{S}_{10.96}$
Q6-038	14.29	n.a.	0.54	0.32	66.70	n.a.	0.00	18.82	100.68	$(\text{Cu}_{4.16}\text{Ag}_{0.05})\Sigma 4.21(\text{Bi}_{5.90}\text{Pb}_{0.05})\Sigma 5.95\text{S}_{10.86}$
Q6-039	14.30	n.a.	0.49	0.39	66.42	n.a.	0.00	18.96	100.56	$(\text{Cu}_{4.14}\text{Ag}_{0.07})\Sigma 4.21(\text{Bi}_{5.87}\text{Pb}_{0.04})\Sigma 5.90\text{S}_{10.89}$
Q6-040	14.26	n.a.	0.51	0.45	66.45	n.a.	0.00	18.88	100.55	$(\text{Cu}_{4.13}\text{Ag}_{0.08})\Sigma 4.21(\text{Bi}_{5.87}\text{Pb}_{0.05})\Sigma 4.92\text{S}_{10.87}$
Mean $n = 10$	13.96	0.38	0.24	0.19	66.67	0.01	0.00	19.04	100.30	$(\text{Cu}_{4.04}\text{Fe}_{0.12}\text{Ag}_{0.03})\Sigma 4.19(\text{Bi}_{5.87}\text{Pb}_{0.02})\Sigma 5.89\text{S}_{10.92}$
σ		1.36	0.04	0.69	0.37	1.54	0.00	0.00	0.38	
Pb-rich hodrušite										
1384-20	12.14	0.04	4.06	n.a.	62.92	0.14	0.00	18.83	98.13	$(\text{Cu}_{3.65}\text{Fe}_{0.01})\Sigma 3.66(\text{Bi}_{5.75}\text{Pb}_{0.37})\Sigma 6.12(\text{S}_{11.20}\text{Sb}_{0.02})\Sigma 11.22$
1384-20b	12.73	0.05	3.62	n.a.	62.14	0.00	0.05	18.72	97.31	$(\text{Cu}_{3.82}\text{Fe}_{0.02})\Sigma 3.84(\text{Bi}_{5.68}\text{Pb}_{0.33})\Sigma 6.01(\text{S}_{11.14}\text{Te}_{0.01})\Sigma 11.15$
1384-21	12.41	0.05	4.39	n.a.	62.68	0.11	0.00	18.93	98.57	$(\text{Cu}_{3.70}\text{Fe}_{0.02})\Sigma 3.72(\text{Bi}_{5.66}\text{Pb}_{0.40})\Sigma 6.08(\text{S}_{11.18}\text{Sb}_{0.02})\Sigma 11.20$
1384-22	12.60	0.07	4.20	n.a.	62.48	0.00	0.09	18.52	97.96	$(\text{Cu}_{3.80}\text{Fe}_{0.02})\Sigma 3.82(\text{Bi}_{5.72}\text{Pb}_{0.39})\Sigma 6.11(\text{S}_{11.06}\text{Te}_{0.01})\Sigma 11.07$
Mean $n = 4$	12.47	0.05	4.07	n.a.	62.56	0.06	0.04	18.75	97.99	$(\text{Cu}_{3.74}\text{Fe}_{0.02})\Sigma 3.76(\text{Bi}_{5.71}\text{Pb}_{0.37})\Sigma 6.08(\text{S}_{11.15}\text{Te}_{0.01})\Sigma 11.16$
σ		0.20	0.00	0.32	---	0.33	0.02	0.01	0.09	
Ingodite										
1383-19	0.01	0.00	0.15	n.a.	71.35	0.00	21.88	5.64	99.03	$\text{Bi}_{1.98}\text{Te}_{1.00}\text{S}_{1.02}$

TABLE 1 (cont'd). CHEMICAL COMPOSITIONS OF THE BISMUTH MINERALS AT EL QUEMADO

	Cu	Fe	Pb	Ag	Bi	Sb	Te	S	Total	Calculated formula
Joséite-A										
1384-11	0.10	0.00	0.00	0.00	80.60	0.00	12.33	6.19	99.22	Cu _{0.01} Bi _{3.99} Te _{1.00} S _{2.00}
Q2-03	0.01	n.a.	0.11	0.00	81.67	n.a.	11.53	6.27	99.60	Bi _{4.04} Te _{0.94} S _{2.02}
Q2-04	0.05	n.a.	0.00	0.03	81.28	n.a.	11.42	6.28	99.07	Bi _{4.03} Te _{0.94} S _{2.03}
Q2-05	0.02	n.a.	0.02	0.01	82.46	n.a.	11.40	6.15	100.06	Bi _{4.08} Te _{0.93} S _{1.99}
Q2-06	0.00	n.a.	0.00	0.00	82.33	n.a.	11.47	6.18	99.98	Bi _{4.08} Te _{0.93} S _{1.99}
Mean <i>n</i> = 5	0.04	0.00	0.03	0.01	81.67	0.00	11.63	6.22	99.58	Bi _{4.04} Te _{0.95} S _{2.01}
σ		0.01	0.00	0.01	0.00	2.36	0.00	0.62	0.01	
Joséite-B										
1383-06	0.04	0.03	0.00	0.00	75.04	0.00	22.44	2.86	100.41	Cu _{0.01} Bi _{4.02} Te _{1.97} S _{1.00}
1383-09	0.02	0.00	0.00	0.00	74.65	0.00	22.10	2.84	99.61	Bi _{4.04} Te _{1.96} S _{1.00}
1383-10	0.07	0.08	0.00	0.00	75.48	0.00	21.18	2.84	99.65	Fe _{0.02} Cu _{0.01} Bi _{4.09} Te _{1.88} S _{1.00}
1383-18	0.10	0.03	0.00	0.00	74.90	0.00	21.97	2.98	99.98	Cu _{0.02} Bi _{4.01} Te _{1.93} S _{1.04}
1384-22	0.09	0.01	0.00	0.00	73.80	0.12	22.43	3.12	99.57	Cu _{0.02} Bi _{3.93} Te _{1.96} (S _{1.08} Sb _{0.01}) _{Σ1.09}
1384-27	0.20	0.00	0.00	0.00	74.77	0.00	21.65	3.06	99.68	Cu _{0.03} Bi _{4.00} Te _{1.90} S _{1.07}
Mean <i>n</i> = 6	0.09	0.03	0.00	0.00	74.77	0.02	21.96	2.95	99.82	Cu _{0.02} Bi _{4.01} Te _{1.93} S _{1.04}
σ		0.02	0.00	0.00	0.00	1.55	0.01	1.18	0.07	
Tetradymite										
Q8-069	0.06	n.a.	0.00	0.02	58.75	n.a.	35.01	4.77	98.60	(Bi _{1.99} Cu _{0.01}) _{Σ2.00} Te _{1.95} S _{1.05}
Q8-070	0.09	n.a.	0.00	0.00	59.40	n.a.	35.48	4.69	99.67	(Bi _{2.00} Cu _{0.01}) _{Σ2.01} Te _{1.96} S _{1.03}
Q8-071	0.10	n.a.	0.00	0.00	59.18	n.a.	35.40	4.66	99.35	(Bi _{2.00} Cu _{0.01}) _{Σ2.01} Te _{1.96} S _{1.03}
Q8-072	0.27	n.a.	0.00	0.09	59.85	n.a.	35.10	4.55	99.87	(Bi _{2.02} Cu _{0.03} Ag _{0.01}) _{Σ2.06} Te _{1.94} S _{1.00}
Q8-073	0.20	n.a.	0.00	0.00	59.82	n.a.	35.25	4.66	99.93	(Bi _{2.01} Cu _{0.02}) _{Σ2.03} Te _{1.95} S _{1.02}
Mean <i>n</i> = 5	0.15		0.00	0.02	59.40		35.25	4.67	99.48	(Bi _{2.00} Cu _{0.02}) _{Σ2.02} Te _{1.95} S _{1.03}
σ	0.03		0.00	0.01	0.86		0.16	0.02		

n: number of analyses.

and ingodite; the amount of chalcopyrite is negligible and commonly isolated from the other minerals or associated with bismuthinite. This array indicates an increase in $f(S_2)$ after the initial precipitation of native bismuth, and an increase, or accumulative concentration, in Te at the final stage.

Native bismuth is a well-known accessory phase locally present in moderately to highly fractionated granitic pegmatites of the Pampean Ranges and elsewhere (*e.g.*, Fersman 1940, Jahns 1953, Černý & Harris 1978, Galliski 1994, Ciobanu & Cook 2002). Bismuthinite occurs in granitic pegmatite systems at higher $f(S_2)$. Some other sulfides, intermetallic compounds, alloys and sulfosalts, especially those belonging to the stannite group, are less common, but nevertheless are encountered locally in some pegmatite fields (Černý *et al.* 2001), and generally are associated with the more evolved rare-element pegmatites (London 2008). In some pegmatites, the compositional diversity of these

phases in general, and of the stannite-group minerals in particular, is remarkable, despite their insignificant quantity (*e.g.*, Černý & Harris 1978).

With a single exception, the samples examined here are the same as those reported by Galliski (1983b). Our study confirmed most of his mineral identifications and expanded the assemblage with the additional species: hodrušite, ingodite, Joséite-A, Joséite-B and tetradymite.

The chemical compositions of the minerals, plotted in the triangles Te–Bi–S and Pb–(Bi + Ag)–(Cu + Fe) (Fig. 4) fit the ideal compositions of their respective phases in general. In detail, there are some differences, especially for hodrušite. In their original description of hodrušite, Koděra *et al.* (1970) found 0.47 wt.% Pb and other components such as Fe and Ag. New analyses led Makovický & MacLean (1972) to believe that Pb is not a constituent of hodrušite. However, new data (Cook & Ciobanu 2003, Topa *et al.* 2003, Jeleň *et al.* 2012) show that Pb, Ag, Fe and Cd are minor components of

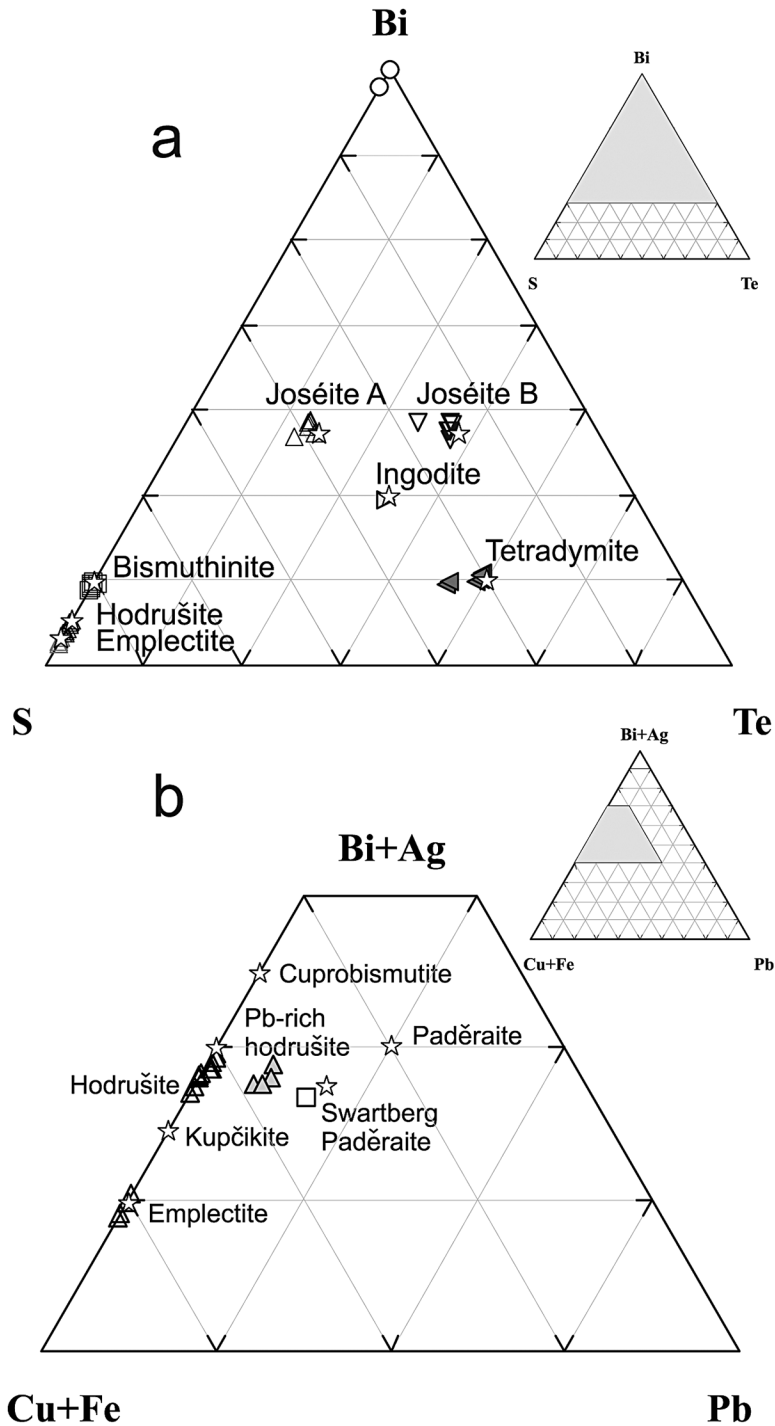


FIG. 4. (a) Te – Bi – S and (b) Pb – Bi + Ag – Cu + Fe (atom.) plots of bismuth minerals at El Quemado; stars represent ideal end-member compositions of the named phases. (b) Hodrušite: open triangles, Pb-rich hodrušite: gray triangles, and emplectite: open triangles. For comparison, the open square represents the composition of paděraite from the Swartberg pegmatite, $Cu_{8.13}Fe_{0.33}Ag_{0.04}Pb_{0.09}Bi_{11.44}S_{21.96}$ (Cook & Ciobanu 2003).

hodrušite from skarns and pegmatites. The low totals of the first batch of analyses of hodrušite from El Quemado were possibly due to the fact that Ag and Cd were not included in the microprobe routine; subsequent analyses showed the presence of up to 0.45 wt.% Ag (Table 1). The Pb-rich hodrušite (3.62 to 4.39 wt.% Pb) at the tips of the hodrušite crystal (Fig. 3g) plots between the fields of hodrušite and paděraite (Fig. 4b). This composition is not known in samples of this homologous series from other deposits (*e.g.*, Ciobanu & Cook 2002, Pieczka & Gołębioska 2012); the highest Pb content found in the literature, 1.59 wt.% Pb, pertains to hodrušite from Ocna de Fier, Romania (Cook & Ciobanu 2003).

Wang's (1994) experimental data on the system Cu – Bi – S show that the assemblage emplectite + bismuthinite + native bismuth is stable between 300° and 200°C. Hodrušite would be stabilized below 200°C, possibly only by incorporation of some impurities. This suggests that the mineral assemblage examined crystallized at relatively low temperatures, and pressures of ~2 to 3 kbar. These physical parameters are consistent with the current understanding of waning hydrothermal stages of consolidation and alteration of rare-element pegmatites (London 1986, Chakoumakos & Lumpkin 1990), and with the conditions of precipitation of sulfide assemblages in other pegmatites (Černý & Harris 1978). The replacement by bismutite and bismite occurred at an even lower temperature, if not supergene, at suppressed $f(S_2)$ and increased $f(CO_2)$.

ACKNOWLEDGEMENTS

The first group of the EMP analyses were performed at the University of Manitoba during a short visit by MFMZ, supported by a scholarship from CONICET of Argentina, followed by extra analyses performed a few years later at the same lab. All of those EMP analyses were financed by NSERC Research and Major Installation Grants to PC and Major Equipment plus Infrastructure Grants to Frank C. Hawthorne. Grants from PIP 319/98 of CONICET and Fundación Antorchas financed the subsequent research in Argentina. Additional analyses were performed at LAMARX, Universidad Nacional de Córdoba, Argentina, financed with PIP 11220090100857/2012 from CONICET and the help of F. Colombo. An earlier version of this paper benefitted from the detailed review and comments of M.K. de Brodtkorb and C. Ciobanu, the comments of associate editor N. Cook and editor R.F. Martin. MFMZ and MÁG are happy to acknowledge the inspiration and insight provided by Petr Černý in our investigations of granitic pegmatites in Argentina.

REFERENCES

- AHLFELD, F. & ANGELELLI, V. (1948): Las Especies Minerales de la República Argentina. *Inst. Geol. Min. (Jujuy), Univ. Nac. Tucumán* **458**.
- AHLFELD, F. & OLSACHER, J.O. (1944): Tetradimita de la Sierra de Córdoba. *Bol. Acad. Nac. Ciencias*. **7**(3), 150-161. Córdoba. Argentina.
- CAMERON, E.N., JAHNS, R.H., MCNAIR, A. & PAGE, L.R. (1949): Internal structure of granitic pegmatites. *Econ. Geol., Monogr.* **2**.
- ČERNÝ, P. & ERCIT, T.S. (2005): The classification of granitic pegmatites revisited. *Can. Mineral.* **43**, 2005-2026.
- ČERNÝ, P. & HARRIS, D.C. (1978): The Tanco pegmatite at Bernic Lake, Manitoba. XI. Native elements, alloys, sulfides, and sulfosalts. *Can. Mineral.* **16**, 625-640.
- ČERNÝ, P., MASAU, M., ERCIT, T.S., CHAPMAN, R. & CHACKOWSKY, L.E. (2001): Stannite and kesterite from the Peerless pegmatite, Black Hills, South Dakota, USA. *J. Czech Geol. Soc.* **46**, 27-33.
- CHAKOUMAKOS, B.C. & LUMPKIN, G.R. (1990): Pressure-temperature constraints on the crystallization of the Harding pegmatite, Taos County, New Mexico. *Can. Mineral.* **28**, 287-298.
- CIOBANU, C.L. & COOK, N.J. (2002): Comparison of primary bismuth association in two southern African pegmatites. In Proc. 11th Quadrennial IAGOD Symp. and Gecongress (Windhoek), CD Extended Abstr. (CD-ROM), Geol. Surv. Namibia.
- COOK, N.J. & CIOBANU, C.L. (2003): Lamellar minerals of the cuprobismutite series and related paděraite: a new occurrence and implications. *Can. Mineral.* **41**, 441-456.
- COOK, N.J., CIOBANU, C.L., WAGNER, T. & STANLEY, C.J. (2007): Minerals of the system Bi-Te-Se-S related to the tetradymite archetype: review of classification and compositional variation. *Can. Mineral.* **45**, 665-708.
- FERSMAN, A.E. (1940): *Pegmatites* (3rd ed.). In Selected Works VI. Acad. Sciences USSR, Moscow, Russia (in Russian; reprinted 1960).
- GALLISKI, M.Á. (1983a): Distrito minero El Quemado, departamentos La Poma y Cachi, Provincia de Salta. El basamento del tramo septentrional de la Sierra de Cachi. *Rev. Asoc. Geol. Arg.* **38**(2), 209-224.
- GALLISKI, M.Á. (1983b): Distrito Minero El Quemado, Dptos La Poma y Cachi, Provincia de Salta. II. Geología de sus pegmatitas. *Rev. Asoc. Geol. Arg.* **38**, 340-380.
- GALLISKI, M.Á. (1994): La Provincia Pegmatítica Pampeana. I. Tipología y distribución de sus principales distritos económicos. *Rev. Asoc. Geol. Arg.* **49**, 99-112.
- GALLISKI, M.Á. (2007): Geoquímica de las Formaciones Puncovicana y Cachi, Sierra de Cachi, Salta. *Discusión. Rev. Asoc. Geol. Arg.* **62**, 475-477.
- GALLISKI, M.Á. & MILLER, C.F. (1989): Petrogénesis de las trondhjemitas de Cachi: condicionamientos impuestos por

- elementos de tierras raras e implicancias tectónicas. *Act. Reunión Geotransectas América del Sur*, 58-62.
- GALLISKI, M.Á., TOSELLI, A.J. & SAAVEDRA, J. (1990): Petrology and geochemistry of Cachi high-alumina trondhjemites, northwestern Argentina. In *Plutonism from Antarctica to Alaska* (S.M. Kay & C. Rapela, eds.). *Geol. Soc. Am., Spec. Pap.* **241**, 91-100.
- JAHNS, R.H. (1953): The genesis of pegmatites. II. Quantitative analysis of lithium-bearing pegmatite, Mora County, New Mexico. *Am. Mineral.* **38**, 1078-1112.
- JELEŇ, S., PRŠEK, J., KOVALENKER, V., TOPA, D., SEJKORA, J., ŠTEVKO, M. & OZDÍN, D. (2012): Bismuth sulfosalts of the cuprobismutite, pavonite and aikinite series from the Rozália mine, Hodruša-Hámre, Slovakia. *Can. Mineral.* **50**, 325-340.
- KODĚRA, M., KUPČÍK, V. & MAKOVICKÝ, E. (1970): Hodrušite, a new sulphosalt. *Mineral. Mag.* **37**, 641-648.
- LONDON, D. (1986): The magmatic-hydrothermal transition in the Tanco rare-element pegmatite: evidence from fluid inclusions and phase equilibrium experiments. *Am. Mineral.* **71**, 376-395.
- LONDON, D. (2008): *Pegmatites*. The Canadian Mineralogist, Special Publication **10**.
- MAKOVICKY, E. & MACLEAN, W.H. (1972): Electron microprobe analysis of hodrušite. *Can. Mineral.* **11**, 504-513.
- PIECZKA, A. & GOŁĘBIOWSKA, B. (2012): Cuprobismutite homologues in granitic pegmatites from Szklarska Poręba, Karkonosze massif, southwestern Poland. *Can. Mineral.* **50**, 313-324.
- POUCHOU, J.L. & PICHOIR, F. (1985): "PAP" $\phi(\rho Z)$ correction procedure for improved quantitative microanalysis. In *Microbeam Analysis* (J.T. Armstrong, ed.). San Francisco Press, San Francisco, California (104-106).
- RIVAS, S. (1969): Estudio espectral y roentgenográfico de tetradimita. *Revista Minera* **29**, 47-48.
- TOPA, D., MAKOVICKY, E. & BALIĆ-ŽUNIĆ, T. (2003): Crystal structures and crystal chemistry of members of the cuprobismutite homologous series of sulfosalts. *Can. Mineral.* **41**, 1481-1501.
- WANG, N. (1994): The Cu-Bi-S system: results from low-temperature experiments. *Mineral. Mag.* **58**, 201-204.

Received May 1, 2004, revised manuscript accepted November 7, 2012.